Slow rupture of frictional interfaces

Yohai Bar Sinai,[1] Efim A. Brener,[1,2] and Eran Bouchbinder[1]

Received 6 December 2011; revised 9 January 2012; accepted 9 January 2012; published 11 February 2012.

[1] The failure of frictional interfaces and the spatiotemporal structures that accompany it are central to a wide range of geophysical, physical and engineering systems. Recent geophysical and laboratory observations indicated that interfacial failure can be mediated by slow slip rupture phenomena which are distinct from ordinary, earthquake-like, fast rupture. These discoveries have influenced the way we think about frictional motion, yet the nature and properties of slow rupture are not completely understood. We show that slow rupture is an intrinsic and robust property of simple non-monotonic rate-and-state friction laws. It is associated with a new velocity scale $c_{\min}$, determined by the friction law, below which steady state rupture cannot propagate. We further show that rupture can occur in a continuum of states, spanning a wide range of velocities from $c_{\min}$ to elastic wave-speeds, and predict different properties for slow rupture and ordinary fast rupture. Our results are qualitatively consistent with recent high-resolution laboratory experiments and may provide a theoretical framework for understanding slow rupture phenomena along frictional interfaces. **Citation:** Bar Sinai, Y., E. A. Brener, and E. Bouchbinder (2012), Slow rupture of frictional interfaces, *Geophys. Res. Lett.*, *39*, L03308, doi:10.1029/2011GL050554.

1. Introduction

[2] Understanding the dynamic processes that govern interfacial failure and frictional sliding, e.g., an earthquake along a natural fault, remains a major scientific challenge. Recently, several geophysical and laboratory observations have pointed to the possibility that stress releasing interfacial slip can be mediated by the propagation of rupture fronts whose velocity is much smaller than elastic wave-speeds [*Rubinstein et al.*, 2004; *Ben-David et al.*, 2010a; *Nielsen et al.*, 2010; *Peng and Gomberg*, 2010].

[3] The nature and properties of these slow rupture fronts, and in particular their propagation velocity, are still not fully understood. The experiments of *Rubinstein et al.* [2004] and *Ben-David et al.* [2010a] clearly demonstrate the existence of a minimal propagation velocity below which no fronts are observed. To the best of our knowledge, no theoretical understanding of this minimal velocity is currently available.

[4] Frictional phenomena are commonly described using phenomenological rate-and-state friction models, see for instance *Dieterich* [1979], *Ruina* [1983], *Baumberger and Caroli* [2006], and *Bizzarri* [2011]. Two possible mechanisms for generating slow rupture events were invoked in this framework. The first involves a non-monotonic dependence of the steady state frictional resistance on slip velocity [*Weeks*, 1993; *Kato*, 2003; *Shibazaki and Iio*, 2003], while the second involves spatial variation of frictional parameters and stress heterogeneities [*Yoshida and Kato*, 2003; *Liu and Rice*, 2005]. The former mechanism is an intrinsic property of the friction law, while the latter mechanism is an extrinsic one. The laboratory measurements of *Rubinstein et al.* [2004] and *Ben-David et al.* [2010a, 2010b], performed on a quasi-2D spatially homogeneous system, may suggest that the second mechanism is not necessary for the existence of slow rupture.

[5] In this study we show that slow rupture naturally emerges in the framework of spatially homogeneous rate-and-state friction models. Our analysis is based on a friction model that includes an elastic response at small shear stresses and a transition to slip above a threshold stress. The model exhibits a crossover from velocity-weakening friction at small slip rates to velocity-strengthening friction at higher slip rates, which we argue to be a generic feature of friction.

[6] The existence of a minimal rupture front velocity $c_{\min}$, which is determined by the friction law and is independent of elastic wave-speeds, is predicted analytically in a quasi-1D limit. We show that there exists a continuum of rupture fronts with velocities ranging from $c_{\min}$ to elastic wave-speeds, in qualitative agreement with recent laboratory measurements [*Ben-David et al.*, 2010a] and possibly consistent with field observations [*Peng and Gomberg*, 2010]. We further show that slow rupture is significantly less spatially localized than ordinary fast rupture. These predictions are corroborated by explicit calculations for a rock (granite) and a polymer (PMMA), demonstrating the existence of slow rupture which is well-separated from ordinary fast rupture. We believe that these results are potentially relevant for slow/silent earthquakes in geological contexts.

2. A Rate-and-State Friction Model

[7] Here we extend the recent ideas of *Brener and Marchenko* [2002], *Braun et al.* [2009], and *Bouchbinder et al.* [2011] into a realistic rate-and-state model of spatially extended frictional interfaces. As is well known, such interfaces are composed of an ensemble of contact asperities whose total area A_r is much smaller than the nominal contact area A_n and which exerts a shear stress τ that resists sliding motion. We decompose τ into an elastic part, emerging from the elastic deformations of contact asperities that are characterized by a coarse-grained stress τ^{el}, and a viscous part τ^{vis}

$$\tau = \tau^{el} + \tau^{vis} = \tau^{el} + \eta\, v^* A\ \mathrm{sgn}(v)\log(1 + |v|/v^*), \quad (1)$$

where η is a viscous-friction coefficient, v is the slip velocity (slip rate), v^* is a low-velocity cutoff scale and $A = A_r/A_n \ll 1$ is the normalized real contact area. The viscous-

[1]Chemical Physics Department, Weizmann Institute of Science, Rehovot, Israel.
[2]Peter Grünberg Institut, Forschungszentrum Jülich, Jülich, Germany.

0094-8276/12/2011GL050554

stress τ^{vis}, which increases with v and scales with A, is usually associated with activated rate processes at asperity contacts (see also discussion by *Baumberger and Berthoud* [1999]). The 1 inside the log ensures a regular behavior in the limit $v \to 0$, but otherwise plays no crucial role in what follows.

[8] The next step is writing down a dynamic evolution equation for τ^{el}. τ^{el} is stored at contact asperities at a rate determined by v and that is proportional to both the interfacial elastic modulus μ_0 and A. It is released as contact asperities are destroyed after slipping over a characteristic distance D (of the order of the size of a contact as in conventional rate-and-state models [*Dieterich*, 1979; *Ruina*, 1983; *Baumberger and Caroli*, 2006]), when the asperity-level stress surpasses a yield-like threshold τ_c. This physical picture is mathematically captured by writing [*Bouchbinder et al.*, 2011]

$$\dot{\tau}^{el} = \mu_0 A v/h - \tau^{el}|v|\theta(\tau/A - \tau_c)/D, \tag{2}$$

where h is the effective height of the asperities. Note that the coarse-grained stress τ is enhanced by a factor $A^{-1} \gg 1$ at the asperities level and that the geometric nature of elastic stress relaxation, emerging from the multi-contact nature of the interface, is captured by the introduction of a spatial length D. The appearance of a Heaviside step function $\theta(\cdot)$ is an outcome of the basic notion of a local static threshold for sliding motion. The evolution law in equation (2) features a reversible elastic response at small shear stresses, $\tau \simeq \tau^{el} = \mu_0 A u/h$, where u is the shear displacement. This elastic response is usually not included in friction models (but see *Bureau et al.* [2000] and *Shi et al.* [2010]), even though it was directly measured experimentally [*Berthoud and Baumberger*, 1998].

[9] To proceed, we write the normalized contact area A in terms of a state variable ϕ as $A(\phi, \sigma) = A_0(\sigma)[1 + b \log(1 + \phi/\phi^*)]$ [*Baumberger and Caroli*, 2006]. Here σ is the (compressive) normal stress and $A_0(\sigma) = \sigma/\sigma_H$, where σ_H is the hardness. The evolution of A is phenomenologically captured by Dieterich's law [*Dieterich*, 1979], extended here by stipulating that the transition from the aging regime ($v = 0$) to the sliding regime ($v \neq 0$) is controlled by the same step function as in equation (2), yielding

$$\dot{\phi} = 1 - \phi|v|\theta(\tau/A - \tau_c)/D, \tag{3}$$

where ϕ is interpreted as the "geometric age" of the contacts. Equations (1)–(3) determine the evolution of $\tau(t)$, i.e., constitute our proposed friction law. We note that if equation (2) is replaced by its steady state solution, $\tau^{el} \sim A(\phi)$, our friction model becomes essentially identical to the conventional rate-and-state model (see also auxiliary material discussion).[1]

[10] Before we proceed we note a very important feature of rate-and-state friction models, which is not specific to the present model. In the absence of persistent sliding, $v = 0$, we have $\phi = t$ and the contact area ages logarithmically $A \propto 1 + b \log(1 + t/\phi^*)$, as is widely observed [*Baumberger and Caroli*, 2006]. The latter form suggests that the logarithmic law is cutoff at short timescales, smaller than ϕ^*, as was directly confirmed experimentally by *Dieterich* [1979], *Nakatani and Scholz* [2006], and *Ben-David et al.* [2010b]. This very same short timescales cutoff manifests itself also under persistent sliding, $v \neq 0$, for which we have $\phi = D/|v|$ and $A \propto 1 + b \log[(1 + D/(\phi^*|v|)]$. In this case, A saturates at a finite value above a typical slip rate of order D/ϕ^* and the fixed-point of equation (2), $\tau^{el} \propto A$, becomes v-independent as well. As a consequence, τ, which usually exhibits a velocity-weakening behavior at small v, becomes velocity-strengthening as the viscous-friction term in equation (1) takes over (see also discussion by *Bizzarri* [2011]). Thus, rate-and-state friction models quantitatively predict a non-monotonic dependence of the steady state sliding friction on the slip rate, an observation that has been largely overlooked in the literature (but see *Weeks* [1993], *Shibazaki and Iio* [2003], *Baumberger and Caroli* [2006], and *Yang et al.* [2008]) and that will play an important role below.

3. Steady State Rupture Fronts

[11] Propagating front solutions exist in multi-stable systems in which one homogeneous (space independent) solution invades another one, giving rise to non-trivial spatiotemporal structures. The spatially homogeneous solutions of equations (1)–(3), as a function of a driving stress τ^d, are shown in Figure 1a. A branch of elastic (static) solutions exists at $v = 0$, where aging effects are neglected, i.e., we assume that $\psi_0 \equiv b \log(1 + t/\phi^*)$ is roughly constant for the timescales relevant for front propagation (essentially we set $t = \phi_0$). A branch of steady sliding solutions with $v > 0$ takes the form

$$f = \tau_{ss}/\sigma \simeq f_0 + \alpha \log(1 + v/v^*) + \beta \log(1 + D/\phi^* v), \tag{4}$$

where $\alpha \equiv \eta\ v^*/\sigma_H$, $\beta \equiv \mu_0 D b/\sigma_H h$, $f_0 \equiv \beta/b$ and f is the steady sliding friction coefficient. Note that we neglected a term of order $\log^2$ in equation (4). As discussed above, steady sliding friction is indeed non-monotonic (when $\alpha < \beta$); friction is velocity-weakening for $v^* \ll v \ll D/\phi^*$ and velocity-strengthening for $v \gg D/\phi^*$, with a minimum at $v_m \simeq (D/\phi^*)(\beta - \alpha)/\alpha$.

[12] At the minimum, we define the friction stress as $\tau_m = \tau_{ss}(v_m)$. Figures 1b–1d present experimental data for a polymer (PMMA), a rock (granite) and paper, where the last two data sets clearly demonstrate the non-monotonic nature of sliding friction, and the first one presumably does not span a sufficiently large range of v's to detect a minimum.

[13] Consider now a homogeneous driving stress τ^d. For $\tau^d < \tau_m$ there exists only one stable homogeneous solution, the elastic (static) one. Upon increasing τ^d above τ_m, three solutions exist: the elastic one with $v = 0$ and two steady sliding solutions, one with $v < v_m$ (typically unstable) and one with $v > v_m$ (typically stable). The critical point $\tau^d = \tau_m$ corresponds to a bifurcation, which suggests a qualitative change in the behavior of the system. At this point we expect steady state propagating rupture, in which a solution with $v \geq v_m$ invades an elastic (static) solution with $v = 0$, to emerge. Denote the propagation velocity of such fronts by c and the one corresponding to $\tau^d = \tau_m$ by $c_{\min}$.

[14] In order to find propagating rupture solutions, and in particular to calculate $c_{\min}$, we need to couple the friction law in equations (1)–(3) to an elastic body. It would not be easy to analytically calculate $c_{\min}$ when the body is a 2D

[1] Auxiliary materials are available in the HTML. doi:10.1029/2011GL050554.

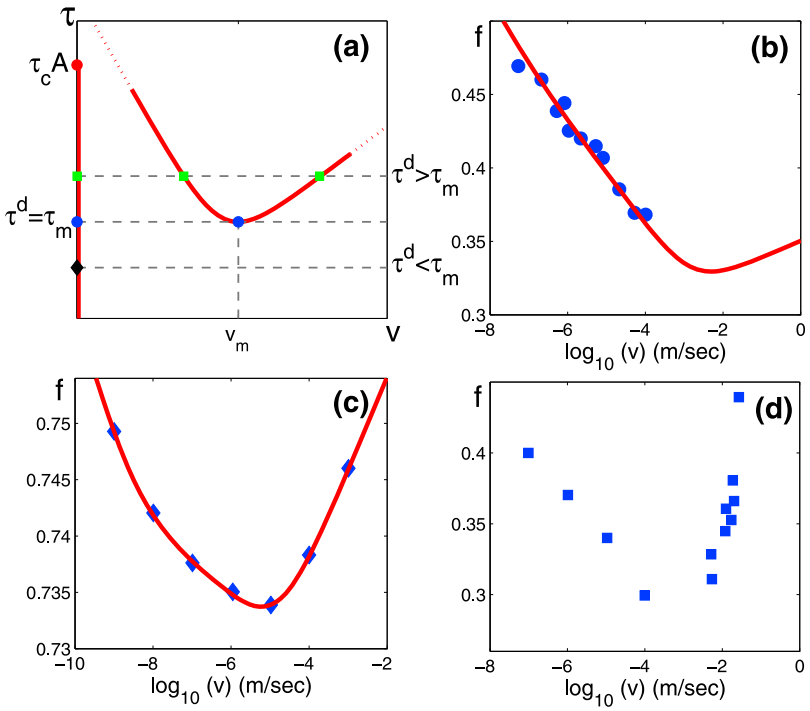

Figure 1. (a) A schematic sketch of the homogeneous solutions of $\tau(v)$. (b) $f(v)$ for PMMA [*Baumberger and Berthoud*, 1999]. The solid line is a fit to equation (4). (c) $f(v)$ for granite with $\sigma = 5$ MPa [*Kilgore et al.*, 1993], in which we added an overall constant. The solid line is a fit to equation (4). (d) $f(v)$ for paper [*Heslot et al.*, 1994].

medium. Therefore, to gain analytic insight into the properties of the steady state fronts, we assume that the height H of the elastic body (say in the y-direction) is much smaller than the spatial scale of variation ℓ of fields along the interface (in the x-direction), i.e., we consider a quasi-1D limit. Under these conditions we obtain (auxiliary material)

$$H\rho\partial_{tt}u(x,t) \simeq H\mu\partial_{xx}u(x,t) + \tau^d - \tau(x,t), \tag{5}$$

where μ is the bulk shear modulus and u is the interfacial shear displacement (slip) that satisfies $\partial_t u = v$. Note that we have omitted constants of order unity in equation (5) and that in the quasi-1D limit both the driving stress τ^d and the friction stress τ do not appear as boundary conditions, but rather as terms in the "bulk" equation.

[15] We now look for steady state propagating solutions of equations (2), (3) and (5) in which all of the fields take the form $g(\xi = x - ct)$, where c is the propagation velocity, such that a sliding solution at $\xi \to -\infty$ propagates into an elastic solution at $\xi \to \infty$. Smoothly connecting these two different solutions around $\xi = 0$ provides solvability conditions that allow the calculation of c. We stress that c must be distinguished from the slip rate v.

[16] $c_{\min}$ is being estimated using a scaling calculation in which the loading τ^d is homogeneous and equals to its threshold value τ_m. A self-consistency constraint on the quasi-1D formulation is $H \ll \ell$, where ℓ is the spatial scale characterizing all of the fields in the front solution (as defined above). We first use $\partial_t = -c\partial_\xi$ to transform equations (2), (3) and (5) into the following set of coupled ordinary differential equations

$$H(\mu/c - c\rho)\partial_\xi v = \tau^d - \tau, \tag{6}$$

$$-c\partial_\xi \tau^{el} = \mu_0 A(\phi,\sigma)v/h - |v|\tau^{el}\theta(\tau/A - \tau_c)/D, \tag{7}$$

$$-c\partial_\xi \phi = 1 - \phi|v|\theta(\tau/A - \tau_c)/D. \tag{8}$$

We stress that the front velocity c in these equations is not a-priori known, but is rather a "nonlinear eigenvalue" of this problem, which is determined from the condition that the spatially-varying propagating solution properly converges to the homogeneous sliding solution at $\xi \to -\infty$ and to the homogeneous elastic solution at $\xi \to \infty$.

[17] A scaling analysis of the above equations (auxiliary material) yields

$$\ell(c_{\min}) \sim Dc_{\min}/v_m \quad \text{and} \quad c_{\min} \sim v_m\sqrt{\frac{\mu H}{\sigma D\Delta f}}, \tag{9}$$

where $\sigma\Delta f$ is the dynamic stress drop, cf. Figure 2 (middle).

[18] Several features of this central result are noteworthy. First, $c_{\min}$ is finite and proportional to v_m. Second, it is independent of inertia, i.e., it does not scale with the elastic wave speed $c_s = \sqrt{\mu/\rho}$ [*Brener and Marchenko*, 2002]. Finally, $c_{\min}$ depends on: (i) the properties of the friction law, e.g., on constitutive parameters such as the viscous-friction coefficient η (through v_m) and the (dimensionless) dynamic stress drop Δf, and on the microscopic geometric quantity D, (ii) the bulk geometry through H, (iii) the normal stress as $\sigma^{-1/2}$ and (iv) the bulk shear modulus μ. We expect these features to remain qualitatively valid independently of the explicit form of the friction law and of dimensionality as long as steady sliding friction exhibits a non-monotonic

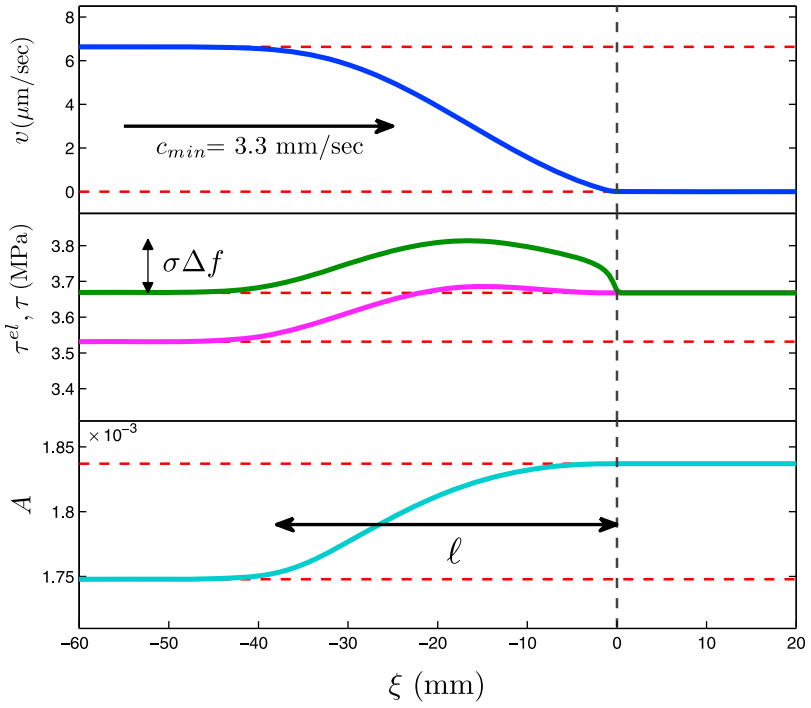

Figure 2. From top to bottom, $v(\xi)$, $\tau(\xi)$ (green), $\tau^{el}(\xi)$ (magenta) and $A(\xi)$ for a steady state rupture mode in granite propagating from left to right at $c_{\min} \approx 3.3$ mm/sec $\ll c_s$. $\sigma\Delta f$ is the dynamic stress drop.

behavior (cf. Figure 1a), as suggested by *Bouchbinder et al.* [2011].

[19] To test the analytic prediction in equation (9), we determine the friction parameters for a rock (granite) and a polymer (PMMA) using various sources and data sets (auxiliary material). In addition, we set $H = 100\mu$m, and $\sigma =$ 5 MPa for granite (as in Figure 1c) and $\sigma = 1$ MPa for PMMA (as by *Ben-David et al.* [2010a, 2010b]). Finally, the state of the interface in the non-flowing region was chosen such that $\psi_0 = 0.06$ (granite) and $\psi_0 = 0.6$ (PMMA). In Figure 2 we show a steady state rupture solution obtained by numerically integrating our model equations for granite. The propagation velocity, $c_{\min} = 3.3$ mm/sec, is about than six orders of magnitude smaller than $c_s \sim 10^3$ m/sec, qualifying it as "slow rupture", and $\ell(c_{\min})$ is on a mm scale, satisfying $H \ll \ell$ as required by self-consistency.

[20] A similar calculation for PMMA (auxiliary material) yields $c_{\min} = 3.8$ m/sec, which is about three orders of magnitude larger than $c_{\min}$ for granite. This is expected since the square root term in equation (9) is not dramatically different for the two materials, but v_m is (cf. Figures 1b and 1c). Recall that $v_m \sim D/\phi^*$ and that D is in the μm scale for both materials (auxiliary material), which imply that the difference emerges from ϕ^*. Indeed, $\phi^* \sim 0.1 - 1$ sec for granite [*Dieterich*, 1979; *Nakatani and Scholz*, 2006] and $\phi^* \sim 10^{-4} - 10^{-3}$ sec for PMMA [*Ben-David et al.*, 2010b].

[21] We test the prediction in equation (9) by each time varying one parameter on the right-hand-side and comparing the prediction to the numerically calculated $c_{\min}$. The results are presented in Figure 3 and exhibit excellent agreement between the analytic prediction and the numerically calculated values of $c_{\min}$ for granite (similar results were obtained for PMMA). This result clearly and directly demonstrates the existence of friction-controlled slow rupture in our model.

4. The Spectrum of Rupture Fronts

[22] The finite velocity scale $c_{\min}$ implies there are no solutions with $c < c_{\min}$, i.e., the existence of a "forbidden" range of velocities in the spectrum of steady state rupture modes [*Bouchbinder et al.*, 2011]. In Figure 4a we show the full spectrum of rupture propagation velocities as a function of $\tau^d \geq \tau_m$ for PMMA (a similar spectrum is obtained for granite, although $c_{\min}$ is much smaller in this case). Indeed, there are no solutions with $c < c_{\min}$ and there exists a continuum of states between $c_{\min}$ and the elastic wave speed c_s. This continuous spectrum seems to be qualitatively similar to recent laboratory measurements [*Ben-David et al.*, 2010a], reproduced here in Figure 4b. These measurements, though not obtained under globally homogeneous loading and were done in 2D, directly demonstrate the existence of a threshold driving stress, a minimal slow rupture velocity and saturation at an elastic wave speed. A detailed quantitative comparison to the experiments requires fully 2D calculations which are currently underway.

[23] Upon increasing τ^d sufficiently above τ_m, rupture travels at a non-negligible fraction of the sound speed and we can no longer neglect the inertial term in equation (6). A scaling analysis (auxiliary material) yields

$$\ell(c \sim c_s) \sim e^{-\tau^d/\alpha\sigma} \ll \ell(c_{\min}). \tag{10}$$

The strong inequality results from the exponential decay of $\ell(c)$ with τ^d in the inertial regime and the typically small value of α ($\sim$0.01). This result predicts that slow rupture

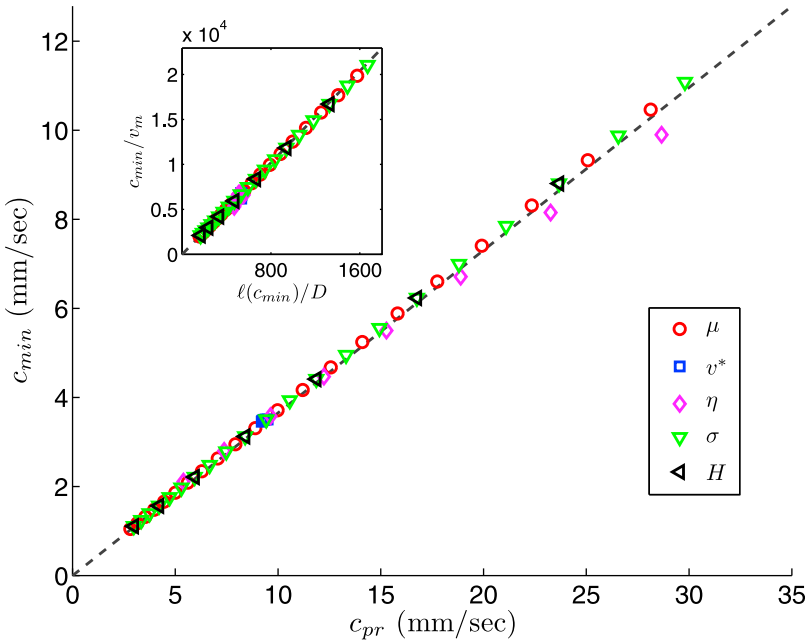

Figure 3. The numerically calculated $c_{\min}$ for granite vs. the analytic prediction appearing on the right-hand-side of equation (9), which we denote here as c_{pr}. (inset) $c_{\min}/v_m$ vs. $\ell(c_{\min})/D$ as obtained in the numerical calculations, cf. equation (9). The dashed lines are guides to the eye.

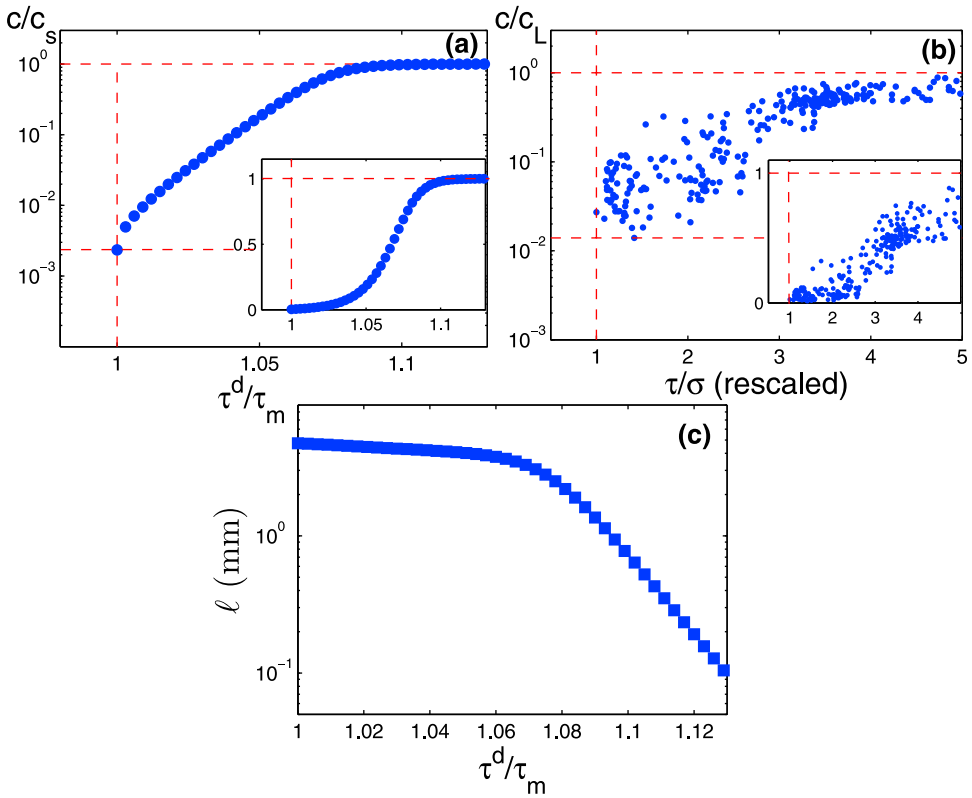

Figure 4. (a) c/c_s vs. τ^d/τ_m for PMMA, under a fixed σ, in semi-log (main) and linear (inset) scales. (b) c/c_L vs. τ/σ in the PMMA experiments of *Ben-David et al.* [2010a] (courtesy of O. Ben-David and J. Fineberg) in semi-log (main) and linear (inset) scales. c_L is the longitudinal wave-speed and τ/σ is rescaled such that the minimal value below which no rupture modes were observed equals unity. $c_{\min}$ here is of the order of 10 m/sec. (c) ℓ vs. τ^d/τ_m for the spectrum in Figure 4a.

is much less spatially localized as compared to ordinary fast rupture. In Figure 4c we test this prediction by plotting ℓ vs. τ^d/τ_m. The numerical results clearly confirm the theoretical prediction, demonstrating that indeed slow rupture is significantly less localized than rupture propagating at elastodynamic velocities. Furthermore, the exponential dependence predicted in equation (10) is quantitatively verified and the slope agrees with $-1/\alpha\sigma$.

5. Summary and Conclusions

[24] Our results, based on a rate-and-state friction law, show that slow rupture is a well-defined and generic state of frictional interfaces. The non-monotonic dependence of the steady state sliding friction on the slip velocity gives rise to a new, friction-controlled, velocity scale $c_{\min}$ below which no steady state rupture can propagate. Furthermore, our analysis demonstrates that rupture states span a continuum, from friction-controlled slow rupture to inertia-limited, earthquake-like, fast rupture [*Peng and Gomberg*, 2010]. One may speculate that transient rupture modes observed under complex, spatially inhomogeneous, conditions are short-lived excitations of these steady rupture states, as was suggested within a specific context by *Bouchbinder et al.* [2011]. If true, steady state rupture fronts may play a role analogous to "normal modes" or "eigenstates" in other dynamical contexts.

[25] The results presented are qualitatively consistent with recent laboratory measurements on PMMA [*Rubinstein et al.*, 2004; *Ben-David et al.*, 2010a], while similar results were obtained for a rock (granite). A quantitative comparison to experimental data requires 2D calculations which are currently underway. We hope to apply our ideas to a concrete geophysical system (e.g., to a slow/silent earthquake) in a future investigation.

[26] **Acknowledgments.** We thank O. Ben-David and J. Fineberg for numerous insightful discussions. EB acknowledges support of the James S. McDonnell Foundation, the Minerva Foundation with funding from the Federal German Ministry for Education and Research, the Harold Perlman Family Foundation and the William Z. and Eda Bess Novick Young Scientist Fund.

[27] The Editor thanks two anonymous reviewers for their assistance in evaluating this paper.

References

Baumberger, T., and P. Berthoud (1999), Physical analysis of the state-and rate-dependent friction law. II. Dynamic friction, *Phys. Rev. B*, *60*(6), 3928–3939.

Baumberger, T., and C. Caroli (2006), Solid friction from stick–slip down to pinning and aging, *Adv. Phys.*, *55*(3–4), 279–348.

Ben-David, O., G. Cohen, and J. Fineberg (2010a), The dynamics of the onset of frictional slip, *Science*, *330*(6001), 211–214.

Ben-David, O., S. M. Rubinstein, and J. Fineberg (2010b), Slip-stick and the evolution of frictional strength, *Nature*, *463*(7277), 76–79.

Berthoud, P., and T. Baumberger (1998), Shear stiffness of a solid–solid multicontact interface, *Proc. R. Soc. London, Ser. A*, *454*(1974), 1615–1634.

Bizzarri, A. (2011), On the deterministic description of earthquakes, *Rev. Geophys.*, *49*, RG3002, doi:10.1029/2011RG000356.

Bouchbinder, E., E. A. Brener, I. Barel, and M. Urbakh (2011), Slow crack-like dynamics at the onset of frictional sliding, *Phys. Rev. Lett.*, *107*(23), 235501.

Braun, O., I. Barel, and M. Urbakh (2009), Dynamics of transition from static to kinetic friction, *Phys. Rev. Lett.*, *103*(1), 194301.

Brener, E. A., and V. I. Marchenko (2002), Frictional shear cracks, *J. Exp. Theor. Phys. Lett.*, *76*, 211–214.

Bureau, L., T. Baumberger, and C. Caroli (2000), Shear response of a frictional interface to a normal load modulation, *Phys. Rev. E*, *62*, 6810–6820.

Dieterich, J. H. (1979), Modeling of rock friction: 1. Experimental results and constitutive equations, *J. Geophys. Res.*, *84*(B5), 2161–2168.

Heslot, F., T. Baumberger, B. Perrin, B. Caroli, and C. Caroli (1994), Creep, stick-slip, and dry-friction dynamics: Experiments and a heuristic model, *Phys. Rev. E*, *49*(6), 4973–4988.

Kato, N. (2003), A possible model for large preseismic slip on a deeper extension of a seismic rupture plane, *Earth Planet. Sci. Lett.*, *216*(1–2), 17–25.

Kilgore, B. D., M. L. Blanpied, and J. H. Dieterich (1993), Velocity dependent friction of granite over a wide range of conditions, *Geophys. Res. Lett.*, *20*(10), 903–906.

Liu, Y., and J. R. Rice (2005), Aseismic slip transients emerge spontaneously in three-dimensional rate and state modeling of subduction earthquake sequences, *J. Geophys. Res.*, *110*, B08307, doi:10.1029/2004JB003424.

Nakatani, M., and C. H. Scholz (2006), Intrinsic and apparent short-time limits for fault healing: Theory, observations, and implications for velocity-dependent friction, *J. Geophys. Res.*, *111*, B12208, doi:10.1029/2005JB004096.

Nielsen, S., J. Taddeucci, and S. Vinciguerra (2010), Experimental observation of stick-slip instability fronts, *Geophys. J. Int.*, *180*(2), 697–702.

Peng, Z., and J. Gomberg (2010), An integrated perspective of the continuum between earthquakes and slow-slip phenomena, *Nat. Geosci.*, *3*(9), 599–607.

Rubinstein, S. M., G. Cohen, and J. Fineberg (2004), Detachment fronts and the onset of dynamic friction, *Nature*, *430*, 1005–1009.

Ruina, A. (1983), Slip instability and state variable friction laws, *J. Geophys. Res.*, *88*(B12), 10,359–10,370.

Shi, Z., A. Needleman, and Y. Ben-Zion (2010), Slip modes and partitioning of energy during dynamic frictional sliding between identical elastic-viscoplastic solids, *Int. J. Fract.*, *162*, 51–67.

Shibazaki, B., and Y. Iio (2003), On the physical mechanism of silent slip events along the deeper part of the seismogenic zone, *Geophys. Res. Lett.*, *30*(9), 1489, doi:10.1029/2003GL017047.

Weeks, J. D. (1993), Constitutive laws for high-velocity frictional sliding and their influence on stress drop during unstable slip, *J. Geophys. Res.*, *98*(B10), 17,637–17,648.

Yang, Z., H. P. Zhang, and M. Marder (2008), Dynamics of static friction between steel and silicon, *Proc. Natl. Acad. Sci. U. S. A.*, *105*, 13,264–13,268.

Yoshida, S., and N. Kato (2003), Episodic aseismic slip in a two-degree-of-freedom block-spring model, *Geophys. Res. Lett.*, *30*(13), 1681, doi:10.1029/2003GL017439.

Y. Bar Sinai and E. Bouchbinder, Chemical Physics Department, Weizmann Institute of Science, 76100 Rehovot, Israel. (yohai.bar-sinai@weizmann.ac.il; eran.bouchbinder@weizmann.ac.il)

E. A. Brener, Peter Grünberg Institut, Forschungszentrum Jülich, D-52425 Jülich, Germany. (e.brener@fz-juelich.de)